

Complex response and polariton-like dispersion splitting in periodic metal nanoparticle chains

A. Femius Koenderink* and Albert Polman

*FOM Institute for Atomic and Molecular Physics AMOLF, Center for Nanophotonics, Kruislaan 407,
1098 SJ Amsterdam, The Netherlands*

(Received 2 June 2006; published 7 July 2006)

We show that guiding of optical signals in chains of metal nanoparticles is subject to a surprisingly complex dispersion relation. Retardation causes the dispersion relation for transverse modes to split in two anticrossing branches, as is common for polaritons. While huge radiation losses occur above the light line, just below the light line the micron-sized loss lengths are much longer than expected. The anticrossing allows one to create highly localized energy distributions in finite arrays that can be tuned via the illumination wavelength. Our results apply to all linear chains of coupled resonant scatterers.

DOI: 10.1103/PhysRevB.74.033402

PACS number(s): 42.79.Gn, 42.25.Fx, 73.22.Lp, 78.67.Bf

Ordered arrays of optically driven metal nanospheres may be used to transport optical signals in structures that are much smaller than the wavelength of light.^{1–5} Coherent transport occurs for frequencies close to the plasmon resonance of a single nanosphere, and is mediated by dipole-dipole coupling between resonant particles on a chain. The transverse width of the guiding structure is only limited by the particle diameter, which is an order of magnitude smaller than the optical wavelength. Metal nanoparticle arrays may therefore allow one to overcome current limitations in the miniaturization of integrated optical devices. Although several experimental and theoretical studies^{1–8} confirm that coupling effects occur in metal nanosphere arrays, no complete picture for the dispersion relation and propagation loss has emerged.

Recent studies indicate that radiation damping, retardation effects and long-range coupling, dramatically affect the loss and dispersion.^{7,8} This necessitates a substantial revision of the original theoretical studies.^{2–4,6} In this paper we calculate the dispersion and loss including all these effects for finite and infinite arrays. Remarkably, retardation causes the dispersion to split into two anticrossing branches for transverse modes. Modes with wave vectors slightly larger than those in the embedding medium have the lowest loss, and allow transport over micrometer distances, well in excess of previous estimates.³ We further show that the anticrossing gives rise to a strongly localized optical response in finite arrays that is very sensitive to the incident wavelength around the anticrossing range. As our calculations are not specific to metallic nanoparticles, our results apply in general to periodic arrays of coupled resonant dipoles, in nano-optics as well as in, e.g., atomic arrays interacting with radiation.^{9–12}

We consider finite and infinite arrays of equally spaced metal nanospheres of radius a , spaced by a center-to-center distance d . A coupled point-dipole approximation is well suited to describe the electromagnetic response of such chains.^{6–8,13} We use the electric field generated by a single dipole $\mathbf{p}e^{-i\omega t}$, oscillating with frequency ω

$$\mathbf{E}(\mathbf{p}, \mathbf{r}, \omega) = \frac{1}{4\pi\epsilon} \left[\left(1 - \frac{i\omega r}{v} \right) \frac{3(\hat{\mathbf{r}} \cdot \mathbf{p})\hat{\mathbf{r}} - \mathbf{p}}{r^3} + \frac{\omega^2 \mathbf{p} - (\hat{\mathbf{r}} \cdot \mathbf{p})\hat{\mathbf{r}}}{v^2} \right] e^{i\omega r/v - i\omega t}, \quad (1)$$

where $\hat{\mathbf{r}}$ is the unit vector pointing from the dipole to the

field point at distance r , $\epsilon = n^2\epsilon_0$ is the permittivity of the homogeneous medium in which the dipole is embedded, and $v = c/n$ is the corresponding speed of light. This form of the electric field fully takes into account retardation effects. The induced dipole moment on a nanosphere equals its polarizability $\alpha(\omega)$ times the local electric field, which is composed of the driving field $\mathbf{E}^{(\text{ext})}e^{-i\omega t}$ and the fields of all the other nanospheres. For the n^{th} nanosphere in a linear chain pointing along $\hat{\mathbf{r}}$ we find

$$\mathbf{p}_n = \alpha(\omega) \left\{ \mathbf{E}_n^{(\text{ext})} + \frac{1}{4\pi\epsilon} \sum_{m \neq n} \left[\left(1 - \frac{i\omega|n-m|d}{v} \right) \frac{3(\hat{\mathbf{r}} \cdot \mathbf{p}_m)\hat{\mathbf{r}} - \mathbf{p}_m}{|n-m|^3 d^3} + \frac{\omega^2 \mathbf{p}_m - (\hat{\mathbf{r}} \cdot \mathbf{p}_m)\hat{\mathbf{r}}}{v^2 |n-m|d} \right] e^{i\omega|n-m|d/v} \right\}. \quad (2)$$

For N dipoles, Eq. (2) represents N inhomogeneous coupled linear equations for the dipole moments \mathbf{p}_n . The resonant material response of the metal nanospheres is captured in the frequency dependence of the polarizability $\alpha(\omega)$. Within the Drude model, the polarizability of a nanosphere is Lorentzian (Ref. 9)

$$\alpha_{\text{Drude}}(\omega) = 4\pi\epsilon \frac{\omega_{SP}^2}{\omega_{SP}^2 - \omega^2 - i\omega\gamma} a^3. \quad (3)$$

Throughout this work, we use values $\gamma = 8.25 \cdot 10^{14} \text{ s}^{-1}$, and $\omega_{SP} = 4.64 \cdot 10^{15} \text{ rad/s}$ appropriate for silver particles in glass ($n=1.5$), as derived from tabulated optical constants in Ref. 14. To maintain the energy balance between extinction, scattering, and absorption it is essential to include radiation damping in the polarizability of each nanosphere by setting the polarizability to (Refs. 7–9, 13, and 15–17)

$$\alpha(\omega) = \left[\frac{1}{\alpha_{\text{Drude}}(\omega)} - \frac{i}{6\pi\epsilon} \frac{\omega^3}{v^3} \right]^{-1}. \quad (4)$$

The importance of retardation effects in the optical behavior of metal nanoparticle chains is evident from Fig. 1(a), where we consider the optical response of a chain of ten nanoparticles of radius 30 nm and spacing 75 nm illuminated by a plane wave incident along the array. We plot the ohmic dissipated power ($\propto |\mathbf{p}_n|^2$) for the first and last sphere in the

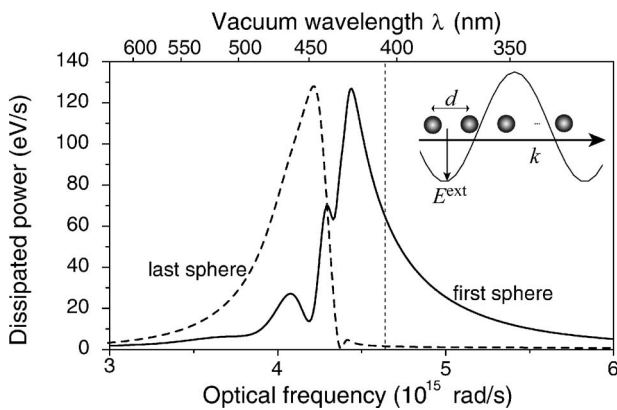


FIG. 1. Excitation by a plane wave along the array causes a localized optical response in finite plasmon arrays (10 Ag particles in glass, radius 30 nm, $d=75$ nm). Depending on driving frequency, the ohmic dissipated power (at 1 V/m incident field) is either concentrated on the first (solid curve), or last sphere (dashed) encountered by the incident beam. Vertical dashes indicate the single particle resonance frequency.

array as a function of the driving optical frequency. In agreement with results reported by Hernández *et al.*,¹³ we find a large asymmetry in the response of the array, which can be tuned via the driving optical frequency. For frequencies below $4.3 \cdot 10^{15}$ rad/s the backmost nanosphere is preferentially excited (dashed line in Fig. 1), i.e., the sphere that is encountered last by the excitation beam. In contrast, this sphere is hardly excited for higher frequencies, for which the front-most sphere is strongly excited (solid curve).

Naively, one expects such strong coupling between the incident wave and the plasmon chain to occur when the plasmon dispersion relation intersects that of the embedding medium (“light line,” $\omega=vk$), i.e., when the incident field is phase matched to the mode in the array. For metal nanoparticle chains a quasistatic model is often used,^{2–4} that is found from Eq. (2) for an infinite number of dipoles, in the limit $\gamma=0$, $c\rightarrow\infty$ and in absence of an external driving field. For the transverse modes that the incident plane wave considered in Fig. 1 can couple to ($\mathbf{p}_m \cdot \hat{\mathbf{r}}=0$), the quasistatic dispersion relation reads

$$\frac{\omega^2}{\omega_{SP}^2} = 1 + \frac{a^3}{d^3} \sum_{j=1}^{\infty} \frac{2 \cos jkd}{j^3},$$

where k is the wave vector. This dispersion relation is plotted in Fig. 2(a) (red solid line). Evidently, the light line (dashed) intersects the quasistatic dispersion relation at a frequency of $4.6 \cdot 10^{15}$ rad/s that does not correspond at all to the frequencies around $4.3 \cdot 10^{15}$ rad/s for which the complex response in Fig. 1 occurs. Furthermore, our exact calculations show that the asymmetric response in Fig. 1 of arrays under plane wave illumination shifts further to the red away from the plasmon resonance as the spacing between particles is increased (data not shown). This shift is in sharp contrast to the rapid d^{-3} decrease of the bandwidth of the quasistatic dispersion relation with increasing particle spacing, that is caused by the strongly reduced overlap of particles with the fields of

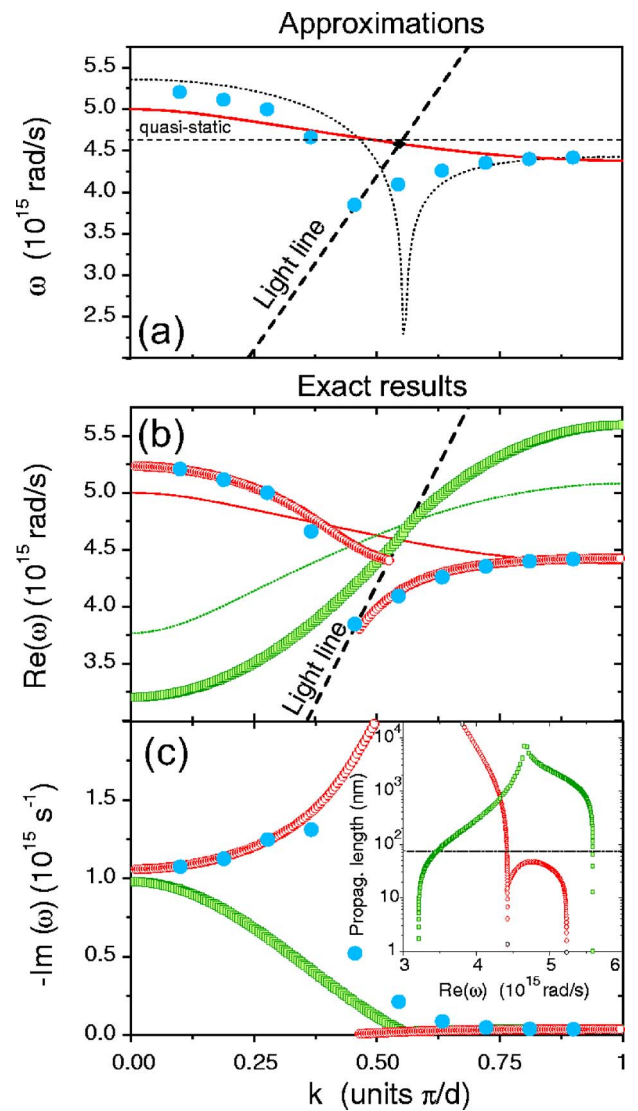


FIG. 2. (Color online) (a) The quasistatic dispersion (solid red curve) for transverse modes intersects the light line ($\omega=vk$, dashed) slightly below the single particle resonance (horizontal dashes). Blue solid circles show the ten normal mode frequencies for an array of ten particles, according to Ref. 7, which agree neither with the quasistatic dispersion, nor with the perturbative result of Ref. 8 (dotted curve). (b) Red open circles (green open squares): real part of the frequency for roots of the exact infinite chain dispersion for transverse (longitudinal) modes. For transverse modes two branches appear that anticross at the light line (dashed). The result agrees well with the finite array dispersion [blue solid circles taken from (a)], but not with the quasistatic approximation (thin curves, dotted green for longitudinal mode). (c) Imaginary part of the frequency for the modes in (b). The damping rate diverges near the light line for transverse modes. Inset in (c): Propagation lengths (amplitude $1/e$ lengths) versus frequency for transverse (red open circles) and longitudinal modes (green open squares). The horizontal dashed line indicates the interparticle spacing d .

their neighbors. We conclude that the asymmetric response in Fig. 1 points at the strong effect of retardation on the array dispersion. Retardation affects the phases of individual nano-

spheres, and thereby the constructive or destructive interference along the chain.

Damping and radiation losses preclude the existence of a dispersion relation which gives solutions of the form $\mathbf{p}_m \propto e^{imkd}$ for real frequencies. However, complex frequency solutions exist, corresponding to the dispersion of damped modes. Recently, several authors have attempted to determine the complex dispersion relation of plasmon chains. Weber and Ford⁷ calculated the complex eigenfrequencies for finite chains of N dipoles, which are frequencies for which the matrix coupling the dipoles in Eq. (2) is singular. A unique wave vector can be assigned to these N modes based on their mode profile.¹⁸ The resulting set of solutions is expected to be an accurate but discrete approximation to the infinite chain dispersion relation, that includes effects of retardation, and ohmic and radiation damping. Reference 7 and the open symbols in Fig. 2(a) show that the resulting dispersion, defined via the real part of the complex frequencies, is dramatically different from the quasistatic result, especially near the light line. Unfortunately, the discrete sampling that is inherent in this approach does not allow one to distinguish between the two distinct scenarios, in which the dispersion relation either has a polariton form with two branches that anticross at the light line, or is a single continuous dispersion relation.

To resolve this ambiguity, we calculate the infinite chain dispersion by inserting $\mathbf{p}_m \propto e^{imkd}$ in Eq. (2), and setting the driving field to zero. Citrin⁸ recently reported that the sums, which exhibit poor convergence for frequencies with negative imaginary parts, can be evaluated in terms of polylogarithms¹⁹ Li_n , resulting in an implicit dispersion relation for transverse modes of the form

$$0 = 1 + \frac{\alpha(\omega)}{4\pi\epsilon d^3} \Sigma(\omega, k) \quad (5)$$

with

$$\begin{aligned} \Sigma(\omega, k) = & [\text{Li}_3(e^{i(\omega/v-k)d}) + \text{Li}_3(e^{i(\omega/v+k)d})] \\ & - \frac{i\omega d}{v} [\text{Li}_2(e^{i(\omega/v-k)d}) + \text{Li}_2(e^{i(\omega/v+k)d})] \\ & - \left(\frac{\omega d}{v} \right)^2 [\text{Li}_1(e^{i(\omega/v-k)d}) + \text{Li}_1(e^{i(\omega/v+k)d})]. \end{aligned} \quad (6)$$

In Ref. 8 this solution was used to approximate the infinite chain dispersion perturbatively by evaluating $\Sigma(\omega, k)$ at the resonance frequency ω_{SP} . The result, plotted as the dotted line in Fig. 2(a), shows that this approximation differs significantly from the quasistatic result and has a deep minimum where the light line crosses the quasistatic dispersion. This minimum is due to the $1/r$ term in the dipole field, which contributes the term $[\text{Li}_1(e^{i(\omega/v-k)d}) + \text{Li}_1(e^{i(\omega/v+k)d})]$ with a logarithmic singularity at the light line. As ω is far from ω_{SP} the validity of this perturbative approach is limited. Therefore we have numerically solved the full dispersion relation to find the complex frequencies ω corresponding to real wave vectors.

Figure 2(b) (solid red dots) shows the dispersion of the real part of the frequency for an infinite chain of $a=30$ nm

radius silver particles spaced by $d=75$ nm, embedded in glass ($n=1.5$). First of all, our result confirms that the deviations of the discrete finite chain result in Fig. 2(a) from the quasistatic result for infinite chains are not due to chain length effects, but to retardation, radiation damping, and ohmic damping. More surprisingly, we find that the dispersion relation for transverse excitations has two branches that anticross at the light line, indicating polariton behavior of the coupled photon-plasmon chain system. Regarding the upper dispersion branch, we note that this branch does extend upwards along the light line, though our numerical algorithm does not identify any clear roots as loss rates become comparable to and exceed the optical frequency. Indeed, the dispersion branch above the light line ($\omega > vk$) is accompanied by huge damping, as gauged by the imaginary part of the frequency plotted in Fig. 2(c). Damping times for this branch are shorter than about one optical cycle, and radiative losses diverge as the light line is approached. The polariton splitting and the different loss regimes for the distinct branches are generic for resonant nanoparticle arrays, and occur for plasmon resonant particles of silver as well as gold over a wide range of particle spacings ($d=50-200$ nm) and radii, and in dielectric hosts ranging from vacuum to high index semiconductors ($n=1-3.5$).

The existence of two dispersion branches that display an avoided crossing is consistent with, but could not be surmised from the finite chain result obtained by Weber and Ford,⁷ and is not represented by the perturbative treatment by Citrin⁸ [dotted line in Fig. 2(a)]. That two disconnected branches appear seems surprising in view of textbook treatments of, e.g., the dispersion of surface plasmon polaritons. Damping causes separate branches to merge when real frequencies but complex k vectors are considered.²⁰ The dispersion of complex frequencies for solutions with real wave vectors, however, displays an avoided crossing, also in the presence of damping. It is important to realize that both types of dispersion relation, i.e., with either frequency or wave vector complex, are relevant, depending on the type of excitation geometry that is used to probe the dispersion.²¹ A treatment in terms of complex frequencies, i.e., normal modes that decay in time, is the natural extension of the normal mode analysis for finite arrays in Ref. 7.

We now turn to the relevance of the exact dispersion relation derived here for proposed applications of metal nanoparticle chains as ultrasmall optical waveguides. Both the group velocities and the damping times in the present calculation are profoundly different from those found in the quasistatic approximation.^{2-4,6} In Fig. 2(c) (inset) we consider the propagation length, defined as the product of the damping time in Fig. 2(c) and the group velocity that we derive from Fig. 2(b). Based on the quasistatic model, the longest propagation lengths are expected near the center of the Brillouin zone.^{3,4} Such predictions as well as extrapolations from $k=0$ measurements⁴ need to be completely revised due to the polariton splitting found here. For transverse excitations, Fig. 2(c) shows that modes above the light line are strongly damped, with damping times comparable to the optical period, and propagation lengths less than the interparticle spacing (open red dots). For modes below the light line ($\omega < vk$), however, no radiative losses occur. Damping rates of

around 10^{13} s $^{-1}$ and group velocities around $0.3c$ provide a frequency window for which propagation lengths above 5 μm are possible.

Applications that require guiding can benefit from longitudinal modes, for which the induced dipoles point along the array. As was also found for finite arrays by Weber and Ford, retardation effects cause the exact dispersion relation [open squares in Fig. 2(b)] to have a doubled bandwidth compared to the quasistatic result (dotted curve). As longitudinal modes do not couple to plane waves that propagate along the array, the intersection with the light line is not associated with diverging loss [Fig. 2(c), open squares] and no splitting of the dispersion relation occurs. In general, guiding benefits from the fact that the group velocity is large over a much wider bandwidth. Below the light line a large frequency window occurs for which the propagation length exceeds 1 μm .

In conclusion, we have presented the dispersion relation of infinite metal nanoparticle chains, fully taking into account the effects of ohmic damping, radiation damping, and retardation. For transverse modes strong coupling to plane waves propagating along the array causes an unexpected splitting of the dispersion into two branches, as is common for polaritons. Propagation lengths just above 1 μm for modes below the light line may allow plasmon chains to be used as very small guiding structures for nanoscale energy transport. With respect to the asymmetric optical response in Fig. 1, it appears that the local excitation intensity set up by an incident plane wave, as gauged by the ohmic dissipation

per sphere, can be used as a sensitive fingerprint of the plasmon chain polariton anticrossing. The sharply defined frequency at which the front-backward asymmetry changes direction, and the peak absorption frequencies for the front and back sphere provide a measure for the location and magnitude of the splitting in the dispersion relation. Such steep frequency edges are sensitive to the refractive index of the medium surrounding the array, and can be useful for, e.g., nanoscale sensing applications. Furthermore, the arrays allow one to create strongly localized energy distributions, that can be varied by tuning the incident plane wave around the anticrossing in the dispersion relation. Such tunable localized energy distributions are useful for, e.g., locally enhancing nonlinear interactions, and nanoscale photolithography with visible wavelengths. Finally we note that these phenomena are general for resonant linear dipole arrays where retardation effects are relevant, and should occur for any chain of coupled resonant dipoles, which also includes systems like quantum dot arrays, or atomic chains that are currently pursued for, e.g., quantum information and computation.^{11,12,22}

We thank L. D. Noordam, W. H. Weber, G. W. Ford, and L. Kuipers for stimulating discussions. This work is part of the research program of the “Stichting voor Fundamenteel Onderzoek der Materie (FOM),” which is financially supported by the “Nederlandse Organisatie voor Wetenschappelijk Onderzoek (NWO).”

*Electronic address: koenderink@amolf.nl

¹M. Quinten, A. Leitner, J. R. Krenn, and F. R. Aussenegg, Opt. Lett. **23**, 1331 (1998).

²M. L. Brongersma, J. W. Hartman, and H. A. Atwater, Phys. Rev. B **62**, R16356 (2000).

³S. A. Maier, P. G. Kik, and H. A. Atwater, Appl. Phys. Lett. **81**, 1714 (2002).

⁴S. A. Maier, M. L. Brongersma, P. G. Kik, and H. A. Atwater, Phys. Rev. B **65**, 193408 (2002).

⁵S. A. Maier, P. G. Kik, H. A. Atwater, S. Meltzer, E. Harel, B. E. Koel, and A. A. G. Requicha, Nat. Mater. **2**, 229 (2003).

⁶S. Y. Park and D. Stroud, Phys. Rev. B **69**, 125418 (2004).

⁷W. H. Weber and G. W. Ford, Phys. Rev. B **70**, 125429 (2004).

⁸D. S. Citrin, Opt. Lett. **31**, 98 (2006).

⁹P. de Vries, D. V. van Coevorden, and A. Lagendijk, Rev. Mod. Phys. **70**, 447 (1998).

¹⁰D. V. van Coevorden, R. Sprik, A. Tip, and A. Lagendijk, Phys. Rev. Lett. **77**, 2412 (1996).

¹¹F. Robicheaux, J. V. Hernández, T. Topcu, and L. D. Noordam, Phys. Rev. A **70**, 042703 (2004).

¹²G. Nienhuis and F. Schuller, J. Phys. B **20**, 23 (1987); J. P. Clemens, L. Horvath, B. C. Sanders, and H. J. Carmichael, Phys. Rev. A **68**, 023809 (2003).

¹³J. V. Hernández, L. D. Noordam, and F. Robicheaux, J. Phys. Chem. B **109**, 15808 (2005).

¹⁴*Handbook of Optical Constants of Solids*, edited by E. D. Palik (Academic, Orlando, FL, 1985).

¹⁵The additional real depolarization correction term $-(\omega/v)^2/(4\pi\epsilon r)$ reported in Ref. 16 is easily included in our formalism.

Additional calculations show that it causes an overall redshift of the dispersion without affecting our conclusions regarding the occurrence of the polariton splitting. This term is specific to finite size scatterers, does not affect the Lorentzian line shape in Eq. (3) to first order¹⁷ and does not occur for other highly polarizable systems like resonant atoms, molecules or quantum dots.

¹⁶M. Meier and A. Wokaun, Opt. Lett. **8**, 581 (1983); K. T. Carron, W. Fluhr, A. Wokaun, and H. W. Lehmann, J. Opt. Soc. Am. B **3**, 420 (1986); K. L. Kelly, E. Coronado, L. L. Zhao, and G. C. Schatz, J. Phys. Chem. B **107**, 668 (2003).

¹⁷S. Zou and G. C. Schatz, J. Chem. Phys. **122**, 097102 (2005).

¹⁸W. H. Weber and G. W. Ford (private communication). Contrary to the result quoted in Ref. 7, more than N poles occur in the coupling matrix for N dipoles. Exactly N poles can be traced to the N modes in the quasistatic limit by their continuous dependence on c and γ .

¹⁹M. H. Lee, Phys. Rev. E **56**, 3909 (1997).

²⁰H. Raether, *Surface Plasmons* (Springer, Berlin, 1988).

²¹A. S. Barker and R. Loudon, Rev. Mod. Phys. **44**, 18 (1972); K. C. Huang, E. Lidorikis, X. Jiang, J. D. Joannopoulos, K. A. Nelson, P. Biesnman, and S. Fan, Phys. Rev. B **69**, 195111 (2004).

²²E. Biolatti, R. C. Iotti, P. Zanardi, and F. Rossi, Phys. Rev. Lett. **85**, 5647 (2000).